

Heme *b* quotas are low in Southern Ocean phytoplankton

Martha Gledhill^{1,2,3,*}, Loes J. A. Gerringa², Patrick Laan², Klaas R. Timmermans²

¹Ocean and Earth Science, University of Southampton, National Oceanography Centre, Southampton SO14 3ZH, UK

²Department of Biological Oceanography, Royal Netherlands Institute for Sea Research, PO Box 59, AB Den Burg (Texel), The Netherlands

³GEOMAR Helmholtz Centre for Ocean Research Kiel, Wischhofstr. 1-3, 24148 Kiel, Germany

ABSTRACT: Heme is the iron-containing prosthetic group of hemoproteins, and is thus required for photosynthesis, respiration and nitrate reduction in marine phytoplankton. Here we report concentrations of heme *b* in Southern Ocean phytoplankton and contrast our findings with those in coastal species. The concentration of particulate heme *b* (pmol l⁻¹) observed at the end of the exponential growth phase was related to the concentration of dissolved iron in the culture media. Small Southern Ocean phytoplankton species (<6 µm in diameter) had heme *b* quotas <1 µmol mol⁻¹ carbon, the lowest yet reported for marine phytoplankton. Heme *b* was also depleted in these species with respect to chlorophyll *a*. We calculated the amount of carbon accumulated per mole of heme *b* per second in our cultures (heme growth efficiency, HGE) and found that small Southern Ocean species can maintain growth rates, even while heme *b* content is reduced. Small Southern Ocean phytoplankton can thus produce more particulate carbon than larger Southern Ocean or small coastal species at equivalent iron concentrations. Combining primary productivity and heme *b* concentrations reported for the open ocean, we found that HGE in natural populations was within the range of our laboratory culture results. HGE was also observed to be higher at open ocean stations characterized by low iron concentrations. Our results suggest that low heme *b* quotas do not necessarily result in reduced growth and that marine phytoplankton can optimize iron use by manipulating the intracellular hemoprotein pool.

KEY WORDS: Iron · *Phaeocystis* sp. · Diatoms · Haptophyte · Limitation · Coastal phytoplankton · Nutrients

Resale or republication not permitted without written consent of the publisher

INTRODUCTION

Iron is an essential nutrient for life but is present at very low concentrations, typically less than 200 pmol l⁻¹, in open ocean surface waters (De Baar & De Jong 2001). As a result of low ambient iron concentrations, open ocean phytoplankton may have lower intracellular iron quotas than coastal species (Sunda et al. 1991, Sunda & Huntsman 1995, Strzepek et al. 2011), optimize their iron use via reduction of iron-rich proteins (Strzepek & Harrison 2004), or exchange iron-containing proteins with non-iron-containing alternatives (Erdner et al. 1999, Peers & Price 2006). Such changes appear to result in increased efficiency of

growth in low-iron environments (Raven 1988, 1990, Strzepek et al. 2011).

The major iron-containing protein pools in phytoplankton are dominated by proteins involved in photosynthesis, nitrate reduction and respiration (Raven 1988, Strzepek & Harrison 2004). Hemoproteins are involved in electron transport and catalysis, and in the control, storage and transport of oxygen and other small molecules (Hogle et al. 2014). Hemes, the prosthetic groups of hemoproteins, contain 1 iron ion per molecule, and many hemoproteins contain multiple hemes (Smith et al. 2010). Hemes are synthesized on the same biosynthetic pathway as chlorophyll and the molecules are related via their common tetrapyr-

*Corresponding author: mgledhill@geomar.de

role ring structure (Tanaka & Tanaka 2007). Free heme is toxic (Espinas et al. 2012), so cellular heme concentrations are tightly regulated via complex feedback mechanisms that control tetrapyrrole synthesis (Tanaka & Tanaka 2007), and via heme oxygenase enzymes, which break down heme into biliverdins and iron (Shekhawat & Verma 2010). The heme iron reservoir could represent as much as 40% of the total intracellular iron pool in marine phytoplankton (Raven 1988, Honey et al. 2013) in circumstances where iron storage is not significant.

Heme can also be a direct source of iron for marine bacteria, and there is evidence to suggest that marine bacteria utilize specific uptake pathways in order to directly access this source of iron (Hopkinson et al. 2008, Roe et al. 2013, Hogle et al. 2014). Hemoprotein concentrations are known to vary in response to iron availability, and intracellular iron concentrations have been shown to be a controlling factor for the biosynthesis of tetrapyrroles (Qi & O'Brian 2002). Diurnal cycling of hemoproteins in diazotrophic cyanobacteria (Saito et al. 2011) and increases in heme oxygenase in red algae (Richaud & Zabulon 1997) have been observed, suggesting that the heme-iron pool may represent a relatively mobile intracellular iron reservoir. Intracellular heme concentrations of marine phytoplankton growing in low-iron environments might therefore be expected to be reduced, with potential impacts on both iron demand and heme-requiring metabolic processes such as photosynthesis or nitrate reduction (Hogle et al. 2014).

Heme *b* (iron protoporphyrin IX) is perhaps the most versatile and ubiquitous heme, and is incorporated into hemoproteins such as the globins, cytochromes, catalase and oxidases. In phytoplankton, heme *b* makes up between 1 and 40% of the total cellular iron pool (Honey et al. 2013). However, no studies on heme abundance or regulation have so far been reported for species isolated from iron-limited regions of the ocean, although Gledhill et al. (2013) have shown that concentrations of heme *b* in particulate material in the iron-limited high latitude North Atlantic and in the Southern Ocean are deplete compared to more iron-replete regions such as the tropical North Atlantic. There is thus a need to examine the heme *b* quotas in phytoplankton species originating from low-iron regions of the ocean to better understand how marine phytoplankton modify their heme *b* protein pool when growing at low-iron concentrations.

The aim of our study was therefore to investigate heme *b* abundance in eukaryotic phytoplankton spe-

cies isolated from the Southern Ocean, one of the lowest iron environments in the ocean. We determined the concentrations of heme *b* accumulated in phytoplankton grown in Southern Ocean seawater at the end of the exponential growth phase. We compared heme *b* to iron concentrations in the cultures, to particulate organic carbon (POC) and to chlorophyll *a* (chl *a*). We utilized the concept of heme growth efficiency (HGE), which, analogous to Raven (1988) and Strzepek et al. (2011), we defined as the moles of carbon fixed per mole of heme *b* per second. In this way we examined the overall impact of reduced heme content on carbon fixation in our phytoplankton cultures. We compared HGE calculated for our Southern Ocean phytoplankton with that calculated from heme *b* concentrations and primary productivity data for 3 sets of previously published field data from contrasting regions—the Celtic Sea (Hickman et al. 2012, Honey et al. 2013), the Scotia Sea (Korb et al. 2012, Gledhill et al. 2013) and the Iceland Basin (Poulton et al. 2010, Gledhill et al. 2013)—to assess the relationship between low heme *b* and phytoplankton productivity in the ocean.

MATERIALS AND METHODS

Phytoplankton growth conditions

Batch cultures of *Phaeocystis antarctica* (CCMP 1871, isolated from the Bellinghousen Sea), *Chaetoceros brevis* (CCMP 163, isolated from the Southern Ocean), *C. dictyota* (Royal Netherlands Institute for Sea Research [NIOZ] culture collection, isolated from the Southern Ocean) and *P. globosa* (NIOZ culture collection, isolated from the North Sea) were grown in triplicate in filtered Southern Ocean seawater (SOs, 0.2 µm, Sartobran, Sartorius) previously collected using trace metal clean sampling techniques from south of the Polar Front from a depth of 2–3 m using a 'fish' towed from RV 'Polastern' (Expedition 18/2, November 2000). Cultures were maintained in acid-washed (1 mol l⁻¹ hydrochloric acid) and Milli-Q-water-rinsed microwave sterilized polycarbonate bottles (Kawachi & Noel 2005). Sample and culture manipulations were carried out in a class 100 laminar flow hood following trace metal clean protocols (Sunda et al. 2005). Southern Ocean seawater was amended with the siderophore desferrioxamine (DFB, 5 nmol l⁻¹, Sigma) or FeCl₃ (5 nmol l⁻¹) to create 3 treatments: SOs, SOs+DFB and SOs+Fe. *P. globosa* and *C. calcitrans* (CCMP 1315, isolated from Japanese coastal waters) were grown in enriched SOs,

which contained added ethylenediaminetetraacetic acid (EDTA, 100 $\mu\text{mol l}^{-1}$), cobalt (50 nmol l^{-1}), molybdenum (100 nmol l^{-1}), copper (20 nmol l^{-1}), manganese (115 nmol l^{-1}), zinc (80 nmol l^{-1}), selenium (10 nmol l^{-1}) and f/2 vitamins. Iron was added separately from a stock solution of 45 $\mu\text{mol l}^{-1}$ FeEDTA to obtain final concentrations of 9, 15, 45 and 150 nmol l^{-1} . All experiments were carried out using a 16 h:8 h light:dark cycle under cool white fluorescent lights at 60 $\mu\text{mol quanta m}^{-2} \text{s}^{-1}$. *P. antarctica*, *C. brevis* and *C. dicaeta* were grown at 4°C, *P. globosa* at 15°C and *C. calcitrans* at 22°C. Cultures were maintained in experimental media for >6 generations prior to experiments. For consistency, and to avoid issues arising from colony formation in both *Phaeocystis* species, growth rates for all species were calculated from the slope of the natural log (F_0 , autofluorescence) obtained for dim-light adapted (15 min) cells using a PAM fluorometer (Walz, Germany) plotted against time. Cell abundance was also monitored daily for *C. brevis*, *C. calcitrans* and *Phaeocystis* sp., by flow cytometry (Accuri C6, BD Biosciences, results not presented). Cultures of *P. globosa*, *P. antarctica* and *C. dicaeta* were examined in 5 ml settling chambers by microscopy (Zeiss Axiovert 25 inverted microscope, results not presented). The PAM fluorometer was used for daily determination of variable versus maximum fluorescence of photosystem II (F_v/F_m). The experiments were terminated and cells harvested when both cell numbers and fluorescence measurements indicated the exponential growth phase was ending.

Analysis of nutrients, dissolved iron and iron speciation in the culture media

Concentrations of the dissolved macronutrients (nitrate + nitrite [termed nitrate for simplicity], phosphate and silicate) were determined on filtered (0.2 μm , 25 mm Acrodisc, Pall) samples using a segmented flow autoanalyzer (Grasshoff et al. 1983; QuAAtro, SEAL Analytical). Samples for nitrate and phosphate were frozen (−20°C) prior to analysis, while samples for silicate were kept at 4°C. The detection limit was typically 0.1, 0.01 and 0.1 $\mu\text{mol l}^{-1}$ for nitrate, phosphate and silicate, respectively. Total dissolved iron was determined by flow injection analysis with chemiluminescence detection on acidified, filtered (0.2 μm , Sartobran, Sartorius) samples according to the methods described in De Baar et al. (2008). Ligand concentrations and the associated conditional stability constants were determined on

filtered samples (0.2 μm) by competitive equilibrium adsorptive cathodic stripping voltammetry using 2-(2-thiazolylazo)-*p*-cresol as the competing ligand (Croot & Johansson 2000). Samples were frozen after collection and defrosted 24 h before analysis. Sample manipulation and data treatment were carried out as described elsewhere (Gerringa et al. 2014).

Analysis of phytoplankton

Samples for POC, particulate organic nitrogen (PON), chl *a* and heme *b* were collected on glass fiber filters (pore size 0.7 μm , Whatman). Filters for POC and PON were ashed prior to use (400°C, 8 h). Filters were stored at −20°C prior to drying (60°C) and analysis with an elemental analyzer (Carlo Erba NA-1500), which was standardized using chitin. Chl *a* was determined by fluorescence against a standard chl *a* solution according to the method of Holm-Hansen et al. (1965).

Heme *b* concentrations were determined in phytoplankton after extraction into ammoniacal detergent (Gledhill 2007). We used octyl β -glucopyranoside as the detergent to allow for determination of heme *b* by mass spectrometry (Gledhill 2014). Samples were stored frozen at −80°C prior to analysis. Heme *b* was quantified, after separation from other pigments, by high performance liquid chromatography–visible spectrophotometry using a diode array detector (DAD) (Gledhill 2007), and by selectively monitoring the major reactant ion (selective reaction monitoring [SRM], specific mass-to-charge ratio [m/z] = 557) produced by collision-induced dissociation of heme *b* (m/z = 616) using an ion trap mass spectrometer (ESI-MS, LTQ-Velos, Thermo Scientific) operating in the positive ion mode (Gledhill 2014). Source conditions were optimized, and the instrument was tuned using standard iron (III) protoporphyrin IX. Masses were calibrated using the automatic instrument calibration procedure and a standard mass calibration solution (Thermo Scientific). Good agreement was observed between the 2 detection methods ($[\text{heme}]_{\text{DAD}} = 1.06 \times [\text{heme}]_{\text{SRM}} + 3.6 \text{ pmol l}^{-1}$, $r^2 = 0.98$, $n = 30$), with the intercept resulting in a potential difference of <0.3% to the heme concentration in *C. calcitrans* cultures. Concentrations derived from SRM are used in the present study, except for *C. calcitrans*, where a problem with the mass spectrometer meant that concentrations were calculated using visible spectrophotometry.

Heme *b* growth efficiency was calculated for phytoplankton in culture. HGE is defined analogous to iron use efficiency after Raven (1988), as the moles of

carbon fixed per mole of heme b per second. In culture, POC represents a good approximation for phytoplankton carbon and HGE was calculated from the growth rate (s^{-1}) and the heme b :POC ratio according to the formula:

$$\text{HGE} = \mu \times \left(\frac{\text{heme } b}{\text{POC}} \right)^{-1} \quad (1)$$

Apparent HGE in 3 areas of the ocean was also calculated by combining previously published heme b concentrations (Gledhill et al. 2013, Honey et al. 2013) with primary productivity (PP) data obtained on the same cruises (Poulton et al. 2010, Hickman et al. 2012, Korb et al. 2012) according to the formula:

$$\text{apparent HGE} = \frac{\text{PP}}{[\text{heme } b]} \quad (2)$$

where PP is given in $\text{mol C m}^{-2} \text{ s}^{-2}$, and [heme b] is given in mol m^{-2} . For field data we add the term 'apparent' as there are several uncertainties in both the determination of primary productivity and heme b due to approximations made in the calculations, methodological constraints and the complexity of community composition (Honey et al. 2013, Juranek & Quay 2013). Integrated heme b concentrations were recalculated to match the depths for the published integrated primary productivity data. Thus, for the Celtic Sea, heme b concentrations were integrated over the whole water column and compared to the median total water column primary productivity given in Table 2 from Hickman et al. (2012). In the Scotia Sea, our stations SSC4, SSP24 and SSP28 had mixed layer depths and integrated chl a concentrations characteristic of 'MID', 'SW-SG' and 'NW-SG' (as defined in Table 2 of Korb et al. 2012), respectively, and heme b was thus integrated to upper mixed layer depths of 43, 61 and 54 m, respectively. To calculate HGE for the Iceland Basin, heme b was integrated to the mixed layer depth given in Table 1 of Poulton et al. (2010).

Statistical analysis of results was carried out using the software package Sigmaplot v.12.5 with ANOVA, or non-parametric ANOVA in cases of non-normal data distributions.

RESULTS

Growth rates

Growth rates and F_v/F_m for the 5 species are presented in Fig. 1. The Southern Ocean species (*Phaeocystis antarctica*, *Chaetoceros brevis* and *C.*

dichaeta) had growth rates of up to 0.5 d^{-1} and F_v/F_m up to 0.5 in SOs or SOs+Fe, similar to values reported previously for Southern Ocean species growing near ambient iron concentrations (Timmermans et al. 2004, Hoffmann et al. 2008, Strzepek et al. 2011). In contrast, *C. calcitrans* repeatedly failed to grow in SOs or SOs+Fe, while *P. globosa* was able to grow in SOs+DFB, SOs and SOs+Fe, albeit with very low growth rates ($0.13\text{--}0.20 \text{ d}^{-1}$) and with significantly reduced F_v/F_m ($p < 0.01$). Consequently, these 2 species were grown in enriched SOs, with added vitamins, EDTA and trace metals, when growth rates of $>0.7 \text{ d}^{-1}$ and $F_v/F_m > 0.6$, i.e. values more typical for

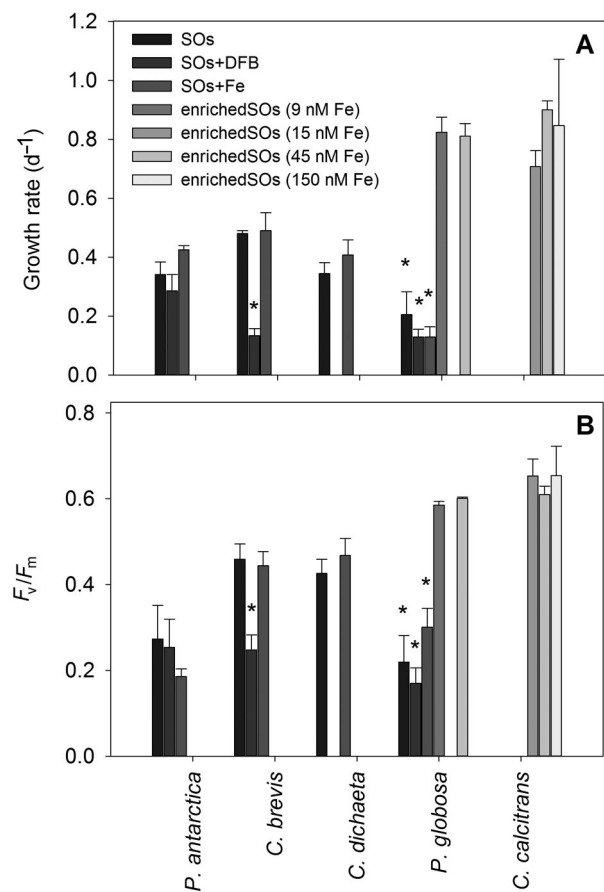


Fig. 1. (A) Growth rates (d^{-1}) and (B) variable versus maximum fluorescence of photosystem II (F_v/F_m) for the Southern Ocean (*Phaeocystis antarctica*, *Chaetoceros brevis* and *C. dichaeata*) and coastal (*P. globosa* and *C. calcitrans*) phytoplankton grown in Southern Ocean seawater (SOs) with added desferrioxamine (DFB), Fe and trace metals plus ethylenediaminetetraacetic acid (EDTA) (enriched SOs). Southern Ocean species were not grown in enriched SOs. Growth in SOs+DFB could not be maintained for *C. dichaeata*. Values are means \pm SD. Significant differences between treatments within species are denoted by asterisks (1-way ANOVA on ranks, * $p < 0.01$)

Table 1. Concentrations of nitrate, phosphate, silicate, particulate organic carbon (POC), particulate organic nitrogen (PON), chlorophyll *a* (chl *a*) and particulate heme *b* observed in cultures of Southern Ocean (*Phaeocystis antarctica*, *Chaetoceros brevis* and *C. dichaeta*) and temperate coastal (*P. globosa* and *C. calcitrans*) phytoplankton species at the end of the experiments. For *P. antarctica*, data for nitrate, phosphate, POC and PON are presented individually ($n = 1$), because of high variability between experimental triplicates. Chl *a* and heme *b* concentrations and all data for other species are given as means \pm SD of experimental triplicates. SOs: Southern Ocean seawater; DFB: desferrioxamine; <dl: less than the detection limit; nd: not determined

	Nitrate ($\mu\text{mol l}^{-1}$)	Phosphate ($\mu\text{mol l}^{-1}$)	Silicate ($\mu\text{mol l}^{-1}$)	POC ($\mu\text{mol l}^{-1}$)	PON ($\mu\text{mol l}^{-1}$)	Chl <i>a</i> (nmol l^{-1})	Heme <i>b</i> (pmol l^{-1})
<i>Phaeocystis antarctica</i>							
SOs	15.3	0.91	nd	69	10	12 \pm 5	8.2 \pm 0.5
	<dl	0.17	nd	190	25		
	5.9	0.4	nd	119	22		
SOs+DFB	10.9	0.46	nd	92	15	12 \pm 5	10 \pm 3
	1.4	0.05	nd	140	32		
	15	0.92	nd	70	13		
SOs+Fe	0.4	<dl	nd	284	22	16 \pm 5	11 \pm 6
	<dl	<dl	nd	114	19		
	<dl	0.1	nd	127	18		
<i>Chaetoceros brevis</i>							
SOs	21.7 \pm 1.9	1.35 \pm 0.05	63.7 \pm 0.8	35 \pm 7	3.7 \pm 0.8	6.6 \pm 2.7	7.7 \pm 3.0
SOs+DFB	25.5 \pm 0.2	1.58 \pm 0.14	65.5 \pm 0.5	6.2 \pm 1.1	1.1 \pm 0.3	1.1 \pm 0.4	2.4 \pm 0.5
SOs+Fe	16.5 \pm 3.4	1.00 \pm 0.11	58.2 \pm 4.4	36 \pm 4	5.9 \pm 1.0	13 \pm 2	13 \pm 3
<i>Chaetoceros dichaeta</i>							
SOs	12.3 \pm 4.2	0.70 \pm 0.27	38.0 \pm 8.9	52 \pm 13	7.3 \pm 1.5	6.9 \pm 1.6	49 \pm 30
SOs+Fe	15.6 \pm 1.9	0.75 \pm 0.14	43.4 \pm 2.3	48 \pm 12	7.3 \pm 2.1	11 \pm 1	47 \pm 6
<i>Phaeocystis globosa</i>							
SOs	24.6 \pm 1.0	1.61 \pm 0.05	nd	16 \pm 4	2.6 \pm 0.3	1.8 \pm 0.6	24 \pm 4
SOs+DFB	24.8 \pm 0.5	1.64 \pm 0.02	nd	14 \pm 3	1.6 \pm 0.1	1.4 \pm 0.2	16 \pm 1
SOs+Fe	22.0 \pm 2.8	1.44 \pm 0.16	nd	16 \pm 4	2.5 \pm 0.6	1.8 \pm 0.5	35 \pm 8
Enriched SOs (9 nM)	<dl	<dl	nd	457 \pm 50	29 \pm 4	49 \pm 3	528 \pm 26
Enriched SOs (45 nM)	<dl	<dl	nd	482 \pm 11	22.3 \pm 1.9	56 \pm 4	800 \pm 200
<i>Chaetoceros calcitrans</i>							
Enriched SOs (15 nM)	<dl	<dl	51.1 \pm 0.4	540 ^a ($n = 1$)	20 ^a ($n = 1$)	61 \pm 7	1170 \pm 80
Enriched SOs (45 nM)	<dl	<dl	50.5 \pm 0.1	560 \pm 34	19 \pm 1	63 \pm 3	1430 \pm 80
Enriched SOs (150 nM)	<dl	<dl	50.9 \pm 2.9	480 \pm 140	21 \pm 1	76 \pm 9	2000 \pm 200

^aTwo samples were lost during analysis

iron-replete conditions) were observed. No attempt was made to grow the Southern Ocean species in enriched SOs.

Culture media nutrient and iron concentrations

Concentrations (means \pm SD) of nitrate, phosphate and silicate in the culture media at the beginning of the experiments were 27.4 \pm 1.0, 1.7 \pm 0.1 and 64.9 \pm 0.7 $\mu\text{mol l}^{-1}$, respectively ($n = 6$). None of the species grown in these experiments completely reduced the nitrate, phosphate or silicate inventories in SOs or SOs+DFB to levels below the detection limit (Table 1). Of the Southern Ocean species, *P. antarctica* consumed the most nitrate, with concentrations

of nitrate depleted to levels below detection in SOs+Fe (Table 1). The amount of nitrate converted to PON in each bottle in experiments with no added iron for *P. antarctica* was rather variable, even though the total nitrogen (i.e. nitrate + PON) calculated for each bottle was close to the concentration of nitrate determined at the start of the experiment (108 \pm 14% for SOs+DFB and 97 \pm 7% for SOs). For cultures of *P. globosa* and *C. calcitrans* grown in enriched SOs, dissolved nitrate was completely removed from the media, and particulate organic nitrogen concentrations were determined to be 95 \pm 16% ($n = 6$) and 82 \pm 0.04% ($n = 7$) of the starting nitrate concentrations, respectively.

Iron concentrations in SOs averaged 0.35 \pm 0.17 nmol l^{-1} ($n = 5$) for the experiments on *C. brevis* and

C. dictyota, and $0.29 \pm 0.01 \text{ nmol l}^{-1}$ ($n = 3$) for experiments on *Phaeocystis* sp. The natural ligand (L_i) concentrations in SOs were very similar to the iron concentration ($0.36 \pm 0.03 \text{ nmol Equivalents Fe l}^{-1}$, $n = 2$), and conditional stability constants ($\log K_{\text{FeL}_i(\text{Fe}^{3+})}^{\text{cond}} = 22.4 \pm 0.01 \text{ mol}^{-1}$, at 20°C) were typical for open ocean ligands (Gledhill & Buck 2012). Iron concentrations were not measured in enriched SOs treatments. Dissolved iron concentrations and speciation were also determined in SOs treatments at the end of experiments on *P. antarctica* (0.33 ± 0.21 , $n = 2$), *C. dictyota* (0.2 ± 0.03 , $n = 3$) and *P. globosa* (0.36 ± 0.31 , $n = 3$). Iron concentrations were thus not significantly reduced during the course of the experiments (t -test, $p < 0.05$). The observed increase in variability was likely indicative of small amounts of iron contamination occurring during the course of the experiment. Similarly, ligand concentrations and stability constants did not change, so that the overall average for ligand concentrations at the time that cells were harvested was $0.24 \pm 0.14 \text{ nmol Eq Fe l}^{-1}$ ($n = 6$) and $\log K_{\text{FeL}_i(\text{Fe}^{3+})}^{\text{cond}}$ was 22.8 ± 0.5 ($n = 6$). A simple ion pairing model (van den Berg 1984) was used to estimate a concentration of approximately 4 pmol l^{-1} inorganically complexed iron (Fe') in SOs.

Heme *b* concentrations

We present here the heme *b* concentrations (i.e. $\text{pmol heme } b \text{ l}^{-1}$ culture medium) at the end of the growth period, in order to relate them to the dissolved iron concentrations in a semi-quantitative mass balance approach. The lowest particulate heme *b* concentrations were observed in cultures of *C. brevis* in SOs+DFB (Fig. 2). In these *C. brevis* cultures, approximately $1.0 \pm 0.5\%$ of the dissolved iron present at the beginning of the experiment was incorporated into heme *b*. Particulate heme *b* concentrations were higher in *C. dictyota* cultures when compared to the other Southern Ocean species. For *C. dictyota* cultured in SOs, heme *b* concentrations represented $14 \pm 9\%$ of the total dissolved iron inventory at the start of the experiments. Heme *b* concentrations for *P. antarctica* and *P. globosa* were intermediate in value between *C. brevis* and *C. dictyota*, and no significant differences were observed between SOs, SOs+DFB and SOs+Fe treatments ($p < 0.01$, ANOVA between treatments within species). Heme *b* concentrations observed in *C. calcitrans* and *P. globosa* cultured in enriched SOs were an order of magnitude higher than heme *b* concentrations observed in unenriched SOs (i.e. cultures grown without added

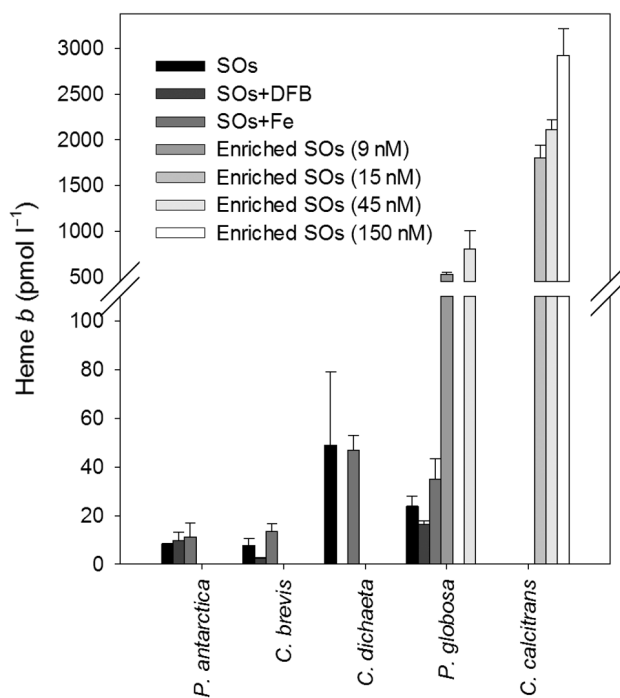


Fig. 2. Heme *b* concentrations (pmol l^{-1}) observed at the end of the exponential phase in Southern Ocean (*Phaeocystis antarctica*, *Chaetoceros brevis* and *C. dictyota*) and coastal (*P. globosa* and *C. calcitrans*) phytoplankton grown in Southern Ocean seawater treatments. Values are means \pm SD. SOs: Southern Ocean seawater; DFB: desferrioxamine

trace metals, EDTA and vitamins), reaching a maximum of $2930 \pm 300 \text{ pmol l}^{-1}$ for *C. calcitrans* grown with 150 nmol l^{-1} iron (Fig. 2). At total iron concentrations of 15 nmol l^{-1} , *C. calcitrans* incorporated $8 \pm 1\%$ of the total iron inventory into heme *b*.

Heme *b* quotas, heme *b*:chl *a* ratios and heme growth efficiency

In this study, heme *b* quotas ($\mu\text{mol heme } b \text{ mol}^{-1} \text{ C}$) and heme *b*:chl *a* ratios did not show significant variability between treatments within species (Fig. 3). However, significant differences in heme *b*:C were observed between species when all treatments were pooled ($p < 0.01$). Heme *b*:C ratios for *C. brevis* and *P. antarctica* were thus significantly lower than those observed for *P. globosa* and *C. calcitrans*, and also lower than those reported previously for other species (Honey et al. 2013). Heme *b*:C ratios reported for *P. antarctica* compare well (overall average $0.08 \pm 0.05 \mu\text{mol mol}^{-1}$) with Fe:C ratios of $2.0\text{--}2.7 \mu\text{mol mol}^{-1}$ previously reported for *P. antarctica* grown at similar iron concentrations (Strzeppek et al. 2011), given that heme *b* has previously been shown to

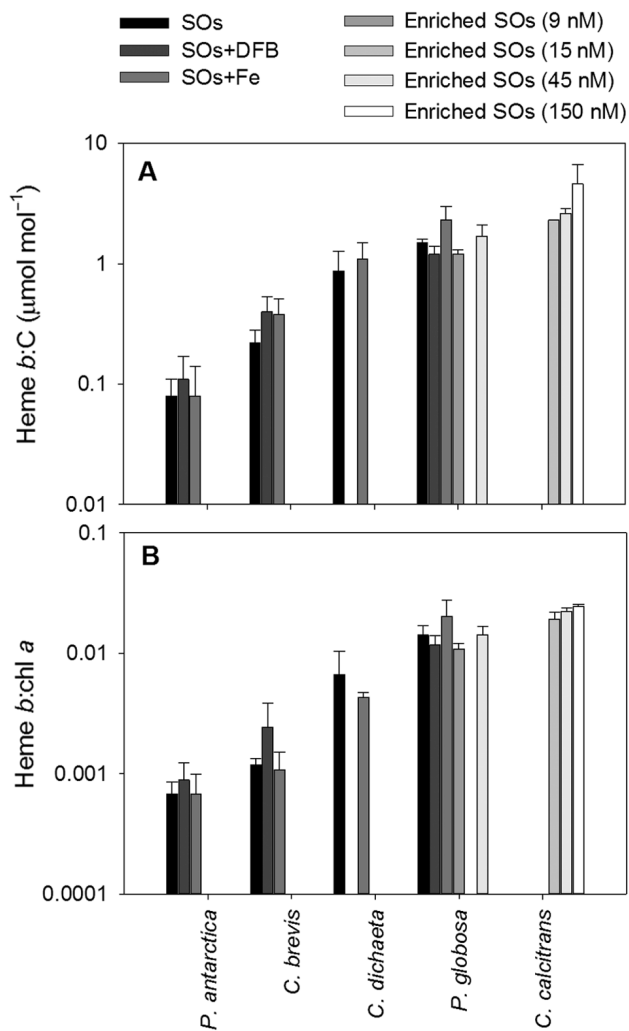


Fig. 3. Intracellular heme *b* concentrations expressed relative to (A) carbon ($\mu\text{mol mol}^{-1}$) in Southern Ocean (*Phaeocystis antarctica*, *Chaetoceros brevis* and *C. dicheata*) and coastal (*P. globosa* and *C. calcitrans*) phytoplankton species and (B) chlorophyll *a* (expressed as the molar ratio) in Southern Ocean and coastal phytoplankton species. Values are means \pm SD. Note log scale on y-axis. SOs: Southern Ocean seawater; DFB: desferrioxamine

make up between 1 and 40% of the total cellular iron pool (Honey et al. 2013). Heme *b*:C and F_v/F_m were weakly correlated ($r = 0.55$, $p < 0.01$, $n = 46$; Fig. 4), as particularly low F_v/F_m was observed for *P. globosa* grown in unenriched SOs treatments. Comparison of heme *b* with particulate organic nitrogen (Table 1) indicated that heme *b*:N ratios increased in treatments where nitrate was completely exhausted.

Heme *b* was also significantly reduced relative to chl *a* for both *P. antarctica* and *C. brevis* compared to *P. globosa* and *C. calcitrans* (Fig. 3B). Heme *b* was observed to be 3 orders of magnitude lower

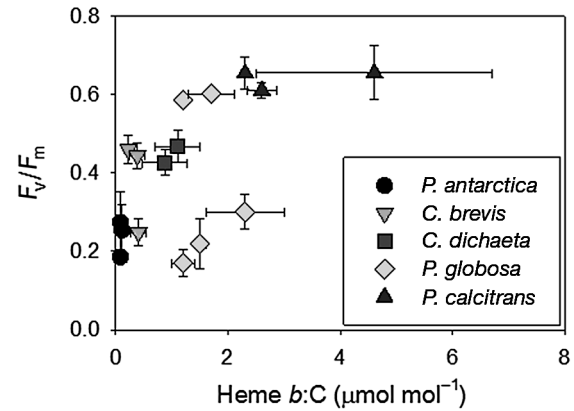


Fig. 4. Relationship between heme *b*:C ($\mu\text{mol mol}^{-1}$) and quantum yield of photosystem II (F_v/F_m) in Southern Ocean (*Phaeocystis antarctica*, *Chaetoceros brevis* and *C. dicheata*) and coastal (*P. globosa* and *C. calcitrans*) phytoplankton species in this study

than chl *a* in these small Southern Ocean species, so that the relative abundances of heme *b* and chl *a* were similar to those observed in particulate material sampled in high-latitude, iron-deplete waters of the North Atlantic and Scotia Sea (Gledhill et al. 2013). Relative abundances of heme *b* and chl *a* in *C. dicheata* were intermediate in value, while the relative abundances of heme *b* and chl *a* in *P. globosa* and *C. calcitrans* were similar to those reported previously for *Phaeodactylum tricornutum*, *Thalassiosira oceanica*, *T. weissflogii* and *Synechococcus* sp. (Honey et al. 2013).

The impact of changes in heme *b* on growth was examined through the calculation of HGE. Comparison within species indicated that a significantly lower HGE was observed for *C. brevis* and *P. globosa* when grown with low iron availability (Fig. 5). When treatments were pooled (omitting treatments with significantly lower HGE), the small Southern Ocean species *P. antarctica* and *C. brevis* were both observed to have significantly higher HGE than *C. calcitrans*, and there was an overall trend of decreasing HGE in the order $P. antarctica > C. brevis > C. dicheata \approx P. globosa \approx C. calcitrans$.

We calculated apparent HGE for the Celtic Sea, a coastal, iron-replete region (Hickman et al. 2012, Honey et al. 2013), the Iceland Basin (Poulton et al. 2010, Gledhill et al. 2013), a high-latitude, seasonally iron-limited region (Nielsdottir et al. 2009), and the Scotia Sea (Korb et al. 2012, Nielsdottir et al. 2012), a productive region of the Southern Ocean. Data used in these calculations are presented in Table 2. Integrated heme *b* concentrations were recalculated to match depths for reported integrated primary pro-

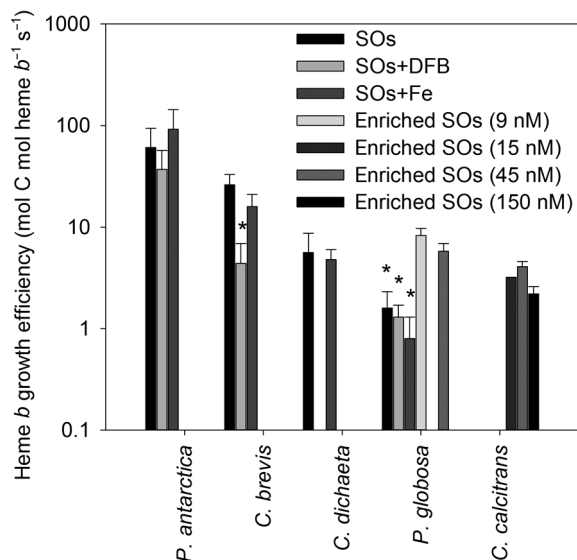


Fig. 5. Heme growth efficiency (HGE, mol C mol heme $b^{-1} s^{-1}$), determined for Southern Ocean (*Phaeocystis antarctica*, *Chaetoceros brevis* and *C. dicaeta*) and coastal (*P. globosa* and *C. calcitrans*) phytoplankton species in our experiments. Values are means \pm SD. Significant differences between treatments within species are denoted by asterisks (1-way ANOVA on ranks, * $p < 0.01$). Note log scale on y-axis. SOs: Southern Ocean seawater; DFB: desferrioxamine

ductivity data (Table 2), and results are presented in Fig. 6. Apparent HGE for the Celtic Sea averaged 2 ± 1 mol C mol heme $b^{-1} s^{-1}$ ($n = 4$), while HGE ranged from 1 to 4.2 mol C mol heme $b^{-1} s^{-1}$ ($n = 3$) in the Scotia Sea and from 1.0 to 27 mol C mol heme $b^{-1} s^{-1}$ ($n = 10$) in the high latitude North Atlantic.

DISCUSSION

We compared heme b concentrations in batch cultures of the Southern Ocean haptophyte *Phaeocystis antarctica* and the diatoms *Chaetoceros brevis* and *C. dicaeta* to those in the temperate coastal species *P. globosa* and *C. calcitrans*. We selected *P. globosa* and *C. calcitrans* because they are similar in size to *P. antarctica* and *C. brevis* (cell volumes of approximately $100 \mu m^3$ for *Phaeocystis* sp., *C. brevis* and *C. calcitrans* as opposed to approximately $4000 \mu m^3$ for *C. dicaeta*), but they were isolated from coastal environments (northwest Europe and Japan, respectively) and thus represented a contrast to the Southern Ocean species with respect to potential iron requirements. It was interesting to note that our coastal species grew very poorly or not at all in unenriched SOs. While the contrasting growth of our Southern Ocean and coastal species in SOs was in

Table 2. Integrated primary productivity, heme b and heme growth efficiency (HGE) calculated from previously published field data. Celtic Sea median integrated primary productivity data for the whole water column were obtained from Hickman et al. (2012). Integrated heme b was calculated from Honey et al. (2013). Scotia Sea primary productivity data were obtained from Korb et al. (2012). We used values for 'MID', 'SW-SG' and 'NW-SG' as these regions had integrated chlorophyll a values that closely corresponded with values we calculated for integrated chlorophyll a at stations SSC4, SSP28 and SSP3, respectively. We adjusted our values for integrated heme b using the upper mixed layer depth given in Korb et al. (2012). Iceland Basin primary productivity data were obtained from Poulton et al. (2010). Integrated heme b from data in Gledhill et al. (2013) was recalculated for depths given in Poulton et al. (2010). See

Fig. 6 for station locations

Station	Primary productivity (mmol C $m^{-2} d^{-1}$)	Heme b (nmol m^{-2})	HGE (mol C mol heme $b^{-1} s^{-1}$)
Celtic Sea			
B21	201	174	1.1
B22	369	217	1.6
OB1	251	276	0.9
U2	273	103	2.6
Scotia Sea			
SSC4	17	270	0.6
SSP28	29	114	2.6
SSP3	233	579	4.2
Iceland Basin			
IB204	17	70	2.8
IB209	11	115	1.1
IB212	23	81	3.2
IB222	10	31	3.7
IB226	41	44	11
IB243	49	76	7.4
IB260	41	19	25
IB274	28	27	12
IB285	65	28	27
IB286	41	59	7.9

accordance with variations in iron requirements reported previously (Timmermans et al. 2005, Hoffmann et al. 2008, Lane et al. 2009, Strzeppek et al. 2011), our experiments do not allow us to identify low iron concentrations as the sole cause for the low growth rates of the coastal species, as multiple trace elements and vitamins were added to the enriched media. Nevertheless, particulate heme b concentrations in our experiments increased with iron concentration (Fig. 2), with up to one-sixth of dissolved iron converted to heme b when iron concentrations were similar to those observed in the ocean. Interestingly, even for *C. calcitrans*, heme b concentrations were $8 \pm 1\%$ of the total iron inventory in cultures containing 15 nM dissolved iron, suggesting that a large pro-

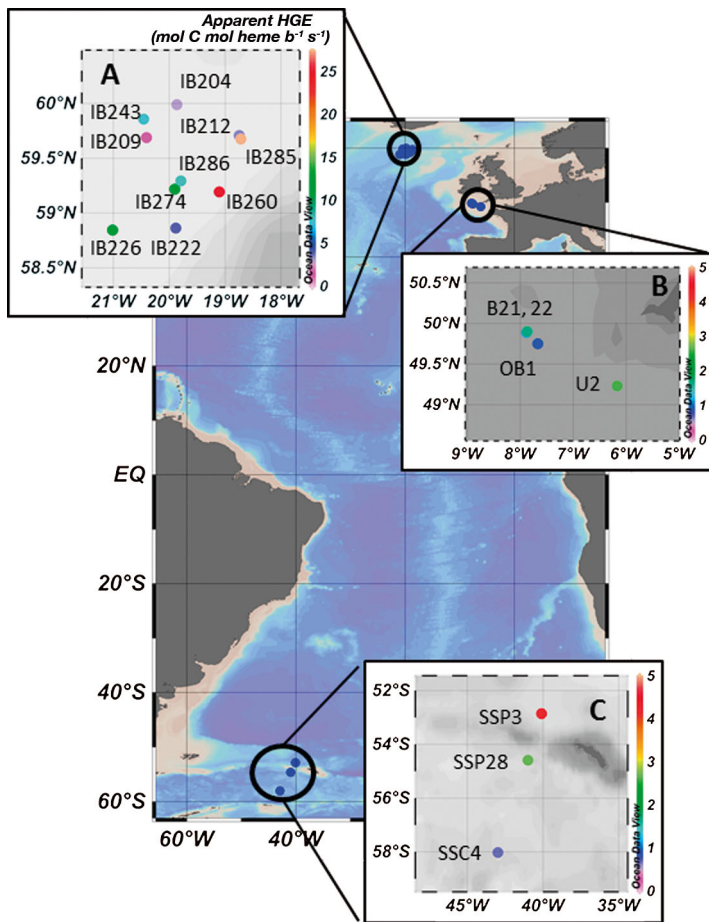


Fig. 6. Apparent heme growth efficiency (HGE, mol C mol heme $b^{-1} s^{-1}$) in (A) the Iceland Basin, (B) the Celtic Sea and (C) the Scotia Sea. HGE was determined for integrated mixed layer depths (Scotia Sea, Iceland Basin) or whole water column depths (Celtic Sea) from previously published productivity data (Poulton et al. 2010, Hickman et al. 2012, Korb et al. 2012) and heme b concentrations (Gledhill et al. 2013, Honey et al. 2013). Note scale change for Iceland Basin. Color bar denotes HGE for all inset figures. Background colors represent bathymetry (light grey: 250–2000 m; dark grey: <250 m)

portion of the total dissolved iron was utilized by this species at this iron concentration.

Closer examination of the different treatments suggests that there are interspecific differences with respect to the influence of the chemical speciation of iron on heme b concentrations. The strong iron chelator DFB reduced growth in *C. brevis* and prevented sustained growth for *C. dictyota*, but made little difference to the amount of heme b produced by *P. antarctica* and *P. globosa* in our experiments. These results agree with previous studies showing that iron in DFB is not universally unavailable to eukaryotic phytoplankton (Strzepek et al.

2011, Shaked & Lis 2012). Furthermore, in our experiments, addition of iron as $FeCl_3$ (SOs+Fe treatments) had only a slight impact on particulate heme b concentrations for all of the species that grew in SOs+Fe (Fig. 2). This is likely a result of losses of the added iron to the bottle walls or as precipitates, as natural ligands were saturated or very close to saturation in SOs. The contrast between heme b concentrations observed with SOs+Fe and those in experiments with enriched SOs highlights the importance of ligands as iron buffers, keeping iron in solution and thus potentially available for uptake (Sunda et al. 2005, Gerringa et al. 2012, Thuróczy et al. 2012).

Macronutrients were underexploited by all species grown in experiments in SOs or SOs+DFB. Enriching SOs with trace metals, a trace metal buffer (EDTA) and vitamins facilitated complete exploitation of macronutrients in the culture media and coincided with order of magnitude increases in heme b concentration. We cannot say with certainty that this increase in macronutrient utilization resulted from the relief of iron limitation alone, as the enriched media involved addition of a suit of trace metals and vitamins in addition to iron. However, an increase in heme b could be directly linked to increased exploitation of nitrate in enriched SOs via an increased ability to undertake cytochrome- b_{557} -dependent assimilatory nitrate reduction. Assimilatory nitrate reduction has previously been shown to be reduced in iron-limited phytoplankton (Timmermans et al. 1994). Furthermore, heme b in assimilatory eukaryotic nitrate reductase is likely to be labile for our extraction protocol (Gledhill et al. 2013, Honey et al. 2013) as the protein is structurally similar to sulfite oxidase (Hille 2013), in which heme b is relatively exposed. However, this potential link between heme b and nitrate reduction is undermined by results from experiments on *P. antarctica*, which indicate that all the available nitrate in SOs+Fe was removed, without any observable increase in heme b concentrations.

Low iron quotas have previously been observed in Southern Ocean phytoplankton (Hassler & Schoemann 2009, Strzepek et al. 2011). However, the abundance of the intracellular content of more specific iron pools has not been widely investigated. Here, we show that small Southern Ocean species also have low heme b quotas (Fig. 3). Furthermore, while heme b was reduced relative to POC in *P. antarctica* and *C. brevis*, chl $a:C$ ratios were not reduced so that the relative abundances of heme b and chl a were similar to those observed in low-iron

regions of the Scotia Sea and Iceland Basin (Gledhill et al. 2013). Low heme *b* relative to chl *a* was not observed in the diatom species examined previously (Honey et al. 2013), but the results obtained for *C. brevis* in the present study indicate that diatoms tolerant to low iron concentrations may also have low heme *b* relative to chl *a*. The present study thus supports previous work that has linked decreases in the abundance of heme *b* relative to chl *a* in the ocean (Honey et al. 2013, Gledhill 2014) to low nutrient availability and the consequent changes in species composition.

Heme *b* is required to fix carbon in eukaryotes as it is a component of the photosystem protein complexes cytochrome b_6/f and photosystem II. Previous work has shown a correlation between the heme *b* quota and F_v/F_m , the quantum yield of photosystem II (Honey et al. 2013). The weaker correlation observed in the present study was highly influenced by the results obtained when *P. globosa* was grown in unenriched SOs. It is possible that *P. globosa* in unenriched SOs was not truly acclimated to the conditions and that this was then reflected in the comparison between F_v/F_m and the heme *b* quota. Nevertheless, the observed trend between F_v/F_m and the heme *b* quota does suggest that, in the majority of treatments, there could be a link between a lower F_v/F_m and the heme *b* quota, and that lower heme *b* may thus impact on growth. In this study, we examined the relationship between growth and heme *b* quotas through calculation of HGE (Eq. 1). Decreasing HGE suggests that low heme *b* quotas have a direct impact on growth, while higher HGE indicates that the heme *b* quota can be optimized. Reduced HGE was observed at low iron concentrations for *C. brevis* and *P. globosa*, suggesting that decreased heme *b* did result in a growth cost. However, growth rates for *P. antarctica* and *C. brevis* in SOs and SOs+Fe were relatively high (Fig. 1) despite the low intracellular heme *b* concentrations, leading to high HGE (Fig. 5) and suggesting that optimization of the heme *b* quota may be a mechanism by which a species can reduce its iron use whilst maintaining growth at low iron concentrations.

Results for HGE could be influenced by the nature of the extraction protocol used for heme *b* determination. Both protein structure and intracellular localization may impact on heme *b* extraction efficiency. The extraction protocol used in the present study has previously been shown to be biased towards heme *b* molecules that are relatively accessible to attack by solvents (Gledhill et al. 2013, Honey et al. 2013). Examination of crystal structures suggests that

heme *b* in the photosystem cytochromes b_6 and b_{559} is at least moderately extractable with our protocol (Stroebel et al. 2003, Müh et al. 2008). Furthermore, the heme *b* in cytochrome b_{559} has been shown to be labile in detergent solution at high pH (Weber et al. 2011). Although we cannot state with confidence which hemoprotein pool is impacted by reductions in heme *b*, our observed variations in HGE indicate that reduced heme *b* does not necessarily result in reduced growth and that individual phytoplankton species are likely to optimize iron use by manipulating the intracellular hemoprotein pool.

It was notable that in our study *P. antarctica* showed a remarkable ability to both fix carbon and utilize nitrate, despite low intracellular heme *b* concentrations. Our results suggest that species such as *P. antarctica* can produce approximately 10 times more particulate carbon than, for example, *P. globosa*, given the same iron and nitrogen resources. Heme *b* makes up an important fraction of the total cellular iron pool. Our work is consistent with a previous study (Strzepek et al. 2011) that also showed an increase in iron use efficiency in small Southern Ocean species such as *P. antarctica*, even though our experiments did not incorporate as long an adaptation time, and our species may not have been fully acclimated to the low iron treatments. Our work thus suggests that a low heme *b* quota and the ability to exploit a wide variety of iron sources likely contribute to the mechanisms by which *P. antarctica* can efficiently exploit iron inputs (Marsay et al. 2014) in areas such as the Ross Sea, where this species can form large blooms, resulting in the drawdown of CO_2 (Tagliabue & Arrigo 2005).

In field samples, heme *b* in non-photosynthesizing plankton could potentially act to decrease apparent HGE, and differences in methodologies used to determine primary productivity could also bias our results (Halsey et al. 2010). However, despite these potential offsets, our calculated apparent HGE obtained from heme *b* concentrations and primary productivity determined for coastal (Celtic Sea) and open ocean (High Latitude North Atlantic [HLNA] and Scotia Sea) regions were within the range calculated in our phytoplankton cultures. In the Scotia Sea, HGE was not as high as that observed for *P. antarctica*, as the Scotia Sea tends to be dominated by diatoms or dinoflagellates (Korb et al. 2010, 2012). The highest HGE was thus observed in the HLNA at stations characterized by iron concentrations <0.05 $nmol\ l^{-1}$, i.e. stations IB285 and IB260 (Gledhill et al. 2013). Thus the lower levels of heme *b* that have been observed in low-iron open-ocean environments

(using this extraction technique) do not necessarily imply low growth or productivity. In fact, increased HGE is necessary in areas with low heme *b* relative to chl *a*, in order to comply with observed correlations between productivity and chl *a* (e.g. Poulton et al. 2010).

In the present study we have shown that small Southern Ocean phytoplankton had low heme *b* quotas. Species with low heme *b* quotas did not necessarily exhibit low growth rates, suggesting that heme *b* quotas were optimized, possibly in order to reduce overall iron requirements. We furthermore compared previously published field data with primary productivity and also found that low heme *b* relative to chl *a* was not necessarily associated with decreased productivity. Our results suggest considerable variability with respect to heme *b* quotas amongst marine phytoplankton in culture, and that this variability may also be observed in the field. Heme *b* quotas could change as a result of optimization of biological iron pools, and could also be influenced by methodological constraints imposed by the extraction protocol. Irrespective of the cause, the finding that a particular iron pool is reduced in phytoplankton growing at low iron concentrations, both in the laboratory and in the field, and that the reduction in this important iron pool does not impact proportionately on carbon accumulation, sheds further light on how marine phytoplankton can adapt to low-iron, open-ocean environments.

Acknowledgements. The authors thank the anonymous reviewers for their constructive comments on the manuscript. The authors also thank A. Noordeloos (NIOZ) for her help with PAM fluorescence and flow cytometry, S. Akbari (University of Southampton, UoS) for his assistance with POC/N analysis and M. Esposito (UoS) for his assistance with the nutrient analysis. M.G. was supported by a Natural Environment Research Council Advanced Fellowship (NE/E013546/1).

LITERATURE CITED

- Croot PL, Johansson M (2000) Determination of iron speciation by cathodic stripping voltammetry in seawater using the competing ligand 2-(2-thiazolylazo)-*p*-cresol (TAC). *Electroanalysis* 12:565–576
- De Baar HJW, De Jong JTM (2001) Distribution, sources and sinks of iron in seawater. In: Turner DR, Hunter KA (eds) *The biogeochemistry of iron in seawater*. Wiley, Chichester, p 123–253
- De Baar HJW, Timmermans KR, Laan P, De Porto HH and others (2008) Titan: a new facility for ultraclean sampling of trace elements and isotopes in the deep oceans in the international Geotraces program. *Mar Chem* 111:4–21
- Erdner DL, Price NM, Doucette GJ, Peleato ML, Anderson DM (1999) Characterization of ferredoxin and flavodoxin as markers of iron limitation in marine phytoplankton. *Mar Ecol Prog Ser* 184:43–53
- Espinás NA, Kobayashi K, Takahashi S, Mochizuki N, Masuda T (2012) Evaluation of unbound free heme in plant cells by differential acetone extraction. *Plant Cell Physiol* 53:1344–1354
- Gerringa LJA, Alderkamp AC, Laan P, Thuróczy CE and others (2012) Iron from melting glaciers fuels the phytoplankton blooms in Amundsen Sea (Southern Ocean): iron biogeochemistry. *Deep Sea Res II* 71-76:16–31
- Gerringa LJA, Rijkenberg MJA, Thuróczy CE, Maas LRM (2014) A critical look at the calculation of the binding characteristics and concentration of iron complexing ligands in seawater with suggested improvements. *Environ Chem* 11:114–136
- Gledhill M (2007) The determination of heme *b* in marine phyto- and bacterioplankton. *Mar Chem* 103:393–403
- Gledhill M (2014) The detection of iron protoporphyrin (heme *b*) in phytoplankton and marine particulate material by electrospray ionisation mass spectrometry — comparison with diode array detection. *Anal Chim Acta* 841: 33–43
- Gledhill M, Buck KN (2012) The organic complexation of iron in the marine environment: a review. *Front Microbiol* 3:69
- Gledhill M, Achterberg EP, Honey DJ, Nielsdottir MC, Rijkenberg MJA (2013) Distributions of particulate heme *b* in the Atlantic Ocean and Southern Ocean — implications for electron transport in phytoplankton. *Global Biogeochem Cycles* 27:1072–1082
- Grasshoff K, Ehrhardt M, Kremling K (1983) *Methods of seawater analysis*. Verlag Chemie, Weinheim
- Halsey KH, Milligan AJ, Behrenfeld MJ (2010) Physiological optimization underlies growth rate-independent chlorophyll-specific gross and net primary production. *Photosynth Res* 103:125–137
- Hassler CS, Schoemann V (2009) Bioavailability of organically bound Fe to model phytoplankton of the Southern Ocean. *Biogeosciences* 6:2281–2296
- Hickman AE, Moore CM, Sharples J, Lucas MI, Tilstone GH, Krivtsov V, Holligan PM (2012) Primary production and nitrate uptake within the seasonal thermocline of a stratified shelf sea. *Mar Ecol Prog Ser* 463:39–57
- Hille R (2013) The molybdenum oxotransferases and related enzymes. *Dalton Trans* 42:3029–3042
- Hoffmann LJ, Peeken I, Lochte K (2008) Iron, silicate, and light co-limitation of three Southern Ocean diatom species. *Polar Biol* 31:1067–1080
- Hogle SL, Barbeau KA, Gledhill M (2014) Heme in the marine environment: from cells to the iron cycle. *Metallomics* 6:1107–1120
- Holm-Hansen O, Lorenzen CJ, Holmes RW, Strickland JDH (1965) Fluorometric determination of chlorophyll. *J Cons Int Explor Mer* 30:3–15
- Honey DJ, Gledhill M, Bibby TS, Legiret FE and others (2013) Heme *b* in marine phytoplankton and particulate material from the North Atlantic Ocean. *Mar Ecol Prog Ser* 483:1–17
- Hopkinson BM, Roe KL, Barbeau KA (2008) Heme uptake by *Microscilla marina* and evidence for heme uptake systems in the genomes of diverse marine bacteria. *Appl Environ Microbiol* 74:6263–6270
- Juranek LW, Quay PD (2013) Using triple isotopes of dissolved oxygen to evaluate global marine productivity. *Annu Rev Mar Sci* 5:503–524

- Kawachi M, Noel MH (2005) Sterilization and sterile techniques. In: Anderson RA (ed) Algal culturing techniques. Elsevier, Beijing, p 65–82
- Korb RE, Whitehouse MJ, Gordon M, Ward P, Poulton AJ (2010) Summer microplankton community structure across the Scotia Sea: implications for biological carbon export. *Biogeosciences* 7:343–356
- Korb RE, Whitehouse MJ, Ward P, Gordon M, Venables HJ, Poulton AJ (2012) Regional and seasonal differences in microplankton biomass, productivity, and structure across the Scotia Sea: implications for the export of biogenic carbon. *Deep-Sea Res II* 59-60:67–77
- Lane ES, Semeniuk DM, Strzepek RF, Cullen JT, Maldonado MT (2009) Effects of iron limitation on intracellular cadmium of cultured phytoplankton: implications for surface dissolved cadmium to phosphate ratios. *Mar Chem* 115:155–162
- Marsay CM, Sedwick PN, Dinniman MS, Barrett PM, Mack SL, McGillicuddy DJ (2014) Estimating the benthic efflux of dissolved iron on the Ross Sea continental shelf. *Geophys Res Lett* 41:7576–7583
- Müh F, Renger T, Zouni A (2008) Crystal structure of cyanobacterial photosystem II at 3.0 angstrom resolution: a closer look at the antenna system and the small membrane-intrinsic subunits. *Plant Physiol Biochem* 46: 238–264
- Nielsdottir MC, Moore CM, Sanders R, Hinz DJ, Achterberg EP (2009) Iron limitation of the postbloom phytoplankton communities in the Iceland Basin. *Global Biogeochem Cycles* 23:GB3001, doi:10.1029/2008GB003410
- Nielsdottir M, Bibby TS, Moore CM, Hinz DJ and others (2012) Seasonal dynamics of iron availability in the Scotia Sea. *Mar Chem* 130-131:62–72
- Peers G, Price NM (2006) Copper-containing plastocyanin used for electron transport by an oceanic diatom. *Nature* 441:341–344
- Poulton AJ, Charalampopoulou A, Young JR, Tarran GA, Lucas MI, Quartly GD (2010) Coccolithophore dynamics in non-bloom conditions during late summer in the central Iceland Basin (July–August 2007). *Limnol Oceanogr* 55:1601–1613
- Qi Z, O'Brian MR (2002) Interaction between the bacterial iron response regulator and ferrochelatase mediates genetic control of heme biosynthesis. *Mol Cell* 9:155–162
- Raven JA (1988) The iron and molybdenum use efficiencies of plant growth with different energy, carbon and nitrogen sources. *New Phytol* 109:279–287
- Raven JA (1990) Predictions of Mn and Fe use efficiencies of phototrophic growth as a function of light availability for growth and of C assimilation pathway. *New Phytol* 116: 1–18
- Richaud C, Zabulon G (1997) The heme oxygenase gene (*pbsA*) in the red alga *Rhodella violacea* is discontinuous and transcriptionally activated during iron limitation. *Proc Natl Acad Sci USA* 94:11736–11741
- Roe KL, Hogle SL, Barbeau KA (2013) Utilization of heme as an iron source by marine *Alphaproteobacteria* in the *Roseobacter* clade. *Appl Environ Microbiol* 79: 5753–5762
- Saito MA, Bertrand EM, Dutkiewicz S, Bulygin VV and others (2011) Iron conservation by reduction of metallo-enzyme inventories in the marine diazotroph *Crocospaera watsonii*. *Proc Natl Acad Sci USA* 108: 2184–2189
- Shaked Y, Lis H (2012) Disassembling iron availability to phytoplankton. *Front Microbiol* 3:123
- Shekhawat GS, Verma K (2010) Haem oxygenase (HO): an overlooked enzyme of plant metabolism and defence. *J Exp Bot* 61:2255–2270
- Smith LJ, Kahraman A, Thornton JM (2010) Heme proteins—diversity in structural characteristics, function, and folding. *Proteins* 78:2349–2368
- Stroebel D, Choquet Y, Popot JL, Picot D (2003) An atypical haem in the cytochrome *b₆f* complex. *Nature* 426: 413–418
- Strzepek RF, Harrison PJ (2004) Photosynthetic architecture differs in coastal and oceanic diatoms. *Nature* 431: 689–692
- Strzepek RF, Maldonado MT, Hunter KA, Frew RD, Boyd PW (2011) Adaptive strategies by Southern Ocean phytoplankton to lesson iron limitation: uptake of organically complexed iron and reduced iron requirements. *Limnol Oceanogr* 56:1983–2002
- Sunda WG, Huntsman SA (1995) Iron uptake and growth limitation in oceanic and coastal phytoplankton. *Mar Chem* 50:189–206
- Sunda WG, Swift DG, Huntsman SA (1991) Low iron requirement for growth in oceanic phytoplankton. *Nature* 351:55–57
- Sunda WG, Price NM, Morel FMM (2005) Trace metal ion buffers and their use in culture studies. In: Anderson RA (ed) Algal culturing techniques. Elsevier, Beijing, p 35–65
- Tagliabue A, Arrigo KR (2005) Iron in the Ross Sea: 1. Impact on CO₂ fluxes via variation in phytoplankton functional group and non-Redfield stoichiometry. *J Geophys Res Oceans* 110:C03009, doi:10.1029/2004JC002531
- Tanaka R, Tanaka A (2007) Tetrapyrrole biosynthesis in higher plants. *Annu Rev Plant Biol* 58:321–346
- Thuróczy CE, Alderkamp AC, Laan P, Gerringa LJA and others (2012) Key role of organic complexation of iron in sustaining phytoplankton blooms in the Pine Island and Amundsen Polynyas (Southern Ocean). *Deep Sea Res II* 71-76:49–60
- Timmermans KR, Stolte W, de Baar HJW (1994) Iron-mediated effects on nitrate reductase in marine phytoplankton. *Mar Biol* 121:389–396
- Timmermans KR, van der Wagt B, de Baar HJW (2004) Growth rates, half-saturation constants, and silicate, nitrate, and phosphate depletion in relation to iron availability of four large, open-ocean diatoms from the Southern Ocean. *Limnol Oceanogr* 49:2141–2151
- Timmermans KR, van der Wagt B, Veldhuis MJW, Maatman A, de Baar HJW (2005) Physiological responses of three species of marine pico-phytoplankton to ammonium, phosphate, iron and light limitation. *J Sea Res* 53: 109–120
- van den Berg CMG (1984) Organic and inorganic speciation of copper in the Irish Sea. *Mar Chem* 14:201–212
- Weber M, Prodohl A, Dreher C, Becker C and others (2011) SDS-facilitated *in vitro* formation of a transmembrane b-type cytochrome is mediated by changes in local pH. *J Mol Biol* 407:594–606